AJNR

Evaluation of a Second-Generation Self-Expanding Variable-Porosity Flow Diverter in a Rabbit Elastase Aneurysm Model

C.N. Ionita, S.K. Natarajan, W. Wang, L.N. Hopkins, E.I. Levy, A.H. Siddiqui, D.R. Bednarek and S. Rudin

AJNR Am J Neuroradiol 2011, 32 (8) 1399-1407
doi: https://doi.org/10.3174/ajnr.A2548
http://www.ajnr.org/content/32/8/1399

ORIGINAL RESEARCH

Evaluation of a Second-Generation Self-Expanding Variable-Porosity Flow Diverter in a Rabbit Elastase Aneurysm Model

C.N. Ionita
S.K. Natarajan
W. Wang
L.N. Hopkins
E.I. Levy
A.H. Siddiqui
D.R. Bednarek
S. Rudin

BACKGROUND AND PURPOSE: The self-expanding V-POD is a second-generation flow-diverting device with a low-porosity PTFE patch on a self-expanding microstent. The authors evaluated this device for the treatment of elastase-induced aneurysms in rabbits.

MATERIALS AND METHODS: Three V-POD types (A, circumferential patch closed-cell stent [$n = 9$]; B, asymmetric patch closed-cell stent [$n = 7$]; and C, asymmetric patch open-cell stent [$n = 4$]) were evaluated by using angiography, conebeam micro-CT, histology, and SEM. Aneurysm flow modifications were expressed in terms of immediate poststent/prestent ratios of maximum CA volume entering the aneurysm dome tracked on procedural angiograms. Flow modifications were correlated with 4 weeks' follow-up angiographic, micro-CT, histologic, and SEM results.

RESULTS: Mechanical stent-deployment difficulties in 4 aneurysms (1 type A; 3 type B) led to suboptimal results and exclusion from analysis. Of the remaining 16 aneurysms, 4-week post-treatment angiograms showed no aneurysm filling in 10 (63%), 3 (~19%) had no filling with a small remnant neck, and 3 (~19%) had <0.25 filling. Successfully treated aneurysms ($n = 16$) demonstrated an immediate poststent/prestent CA maximum volume ratio of 0.13 ± 0.18% (0.0%–0.5%). Favorable contrast-flow modification on immediate angiography after deployment correlated significantly with aneurysm occlusion on follow-up angiography, micro-CT, and histology. The occlusion percentage derived from micro-CT was 96 ± 6.8%. Histology indicated advanced healing (grade ≥3) in the aneurysm dome in 13 of 16 cases. SEM revealed 15 of 16 stents in an advanced state of endothelialization.

CONCLUSIONS: This study showed the feasibility and effectiveness of V-POD for aneurysm healing in a rabbit elastase model.

ABBREVIATIONS: AVS = asymmetric vascular stents; CA = contrast agent; ECM = extracellular matrix; IA = intracranial aneurysm; PTFE = polytetrafluoroethylene; SEM = scanning electron microscopy; V-POD = variable-porosity flow diverter

Ample evidence exists that IA development is due to altered hemodynamics at the parent vessel–aneurysm ostium.[1-3] Endovascular flow-diversion technology[3-6] aims to redirect flow away from the aneurysm ostium, thus reconstructing the parent vessel (via an internal endovascular aneurysmal segment bypass) without the use of endosaccular occlusive devices (ie, coils). Flow-diverting stents change the physiology by reducing aneurysm inflow jets, vorticity, and wall shear stress and providing a scaffold and stimulus for neointimal tissue formation across the aneurysm ostium, thereby altering the biology of the aneurysm–parent vessel complex.[3-6]

Currently tested flow-diverting devices are uniform-porosity high-surface-area-coverage braided stents designed to provide enough flow redirection and endovascular remodeling to induce aneurysm thrombosis with or without the use of additional endosaccular occlusive devices. Large or giant aneurysm size or the presence of intra-aneurysmal thrombus, both of which are factors typically associated with coil-treated aneurysm recurrence, do not appear to be issues with flow-diverting devices. The theoretic basis behind flow-diverting devices is that once the diseased segment is reconstructed and the device is fully endothelialized,[7] the aneurysm and the diseased vessel segment may be considered "definitively" treated, with the typical aneurysm recurrence or regrowth mechanisms being essentially eliminated. The current experience with flow-diverting devices is very limited, and this concept needs to be proved by further studies. In addition, as a purely extrasaccular treatment strategy, no direct catheterization or aneurysm sac manipulation is required, possibly reducing the likelihood of procedural rupture and potentially improving the safety of endovascular IA treatment, especially in small blisterlike aneurysms.

Although it has been shown that flow-diverter pores are

Received September 24, 2010; accepted after revision January 6, 2011.

From the Departments of Radiology (C.N.I., L.N.H., E.I.L., A.H.S., D.R.B., S.R.), Neurosurgery (S.K.N., L.N.H., E.I.L., A.H.S., S.R.), Physiology and Biophysics (S.R., W.W.), Mechanical and Aerospace Engineering (S.R.), and Toshiba Stroke Research Center (C.N.I., S.K.N., W.W., L.N.H., E.I.L., A.H.S., D.R.B., S.R.), School of Medicine and Biomedical Sciences, University at Buffalo, State University of New York, Buffalo, New York; and Department of Neurosurgery (S.K.N., L.N.H, E.I.L., A.H.S.), Millard Fillmore Gates Hospital, Kaleida Health, Buffalo, New York.

This work was supported by NIH grants R01NS43924 and R01EB002873 and Toshiba Medical Systems.

C.N.I. and S.K.N. are co-first authors.

This study was conducted at the Toshiba Stroke Research Center. Procedures were approved by the Institutional Animal Care and Use Committee of the State University of New York at Buffalo and conducted according to Animal Welfare Act guidelines.

Please address correspondence to Stephen Rudin, PhD, Toshiba Stroke Research Center, University at Buffalo, State University of New York, 3425 Main St, Buffalo NY 14214; e-mail srudin@buffalo.edu

Indicates open access to non-subscribers at www.ajnr.org

http://dx.doi.org/10.3174/ajnr.A2548

large enough to allow continued perfusion of branch vessels and perforators,[3] perforator and branch occlusion has been reported, with neurologic deficits.[8] Use of these flow devices for the treatment of basilar bifurcation aneurysms caused complications in 25% of cases due to late ischemic events affecting perforating arteries that occurred after flow diverter implantation.[9-11] In addition, postprocedural aneurysm rupture has been observed with low-porosity flow diverters.[12] These complications could be avoided, theoretically, by having a device with variable porosity, with low porosity at the aneurysm ostium for flow diversion and high porosity at other regions to preserve perforators and branch vessels.

The concept of using AVS has previously been reported.[4,5] These devices are high-porosity balloon-mounted stents containing an asymmetric low-porosity patch and are deployed so that the patch covers the defect in the parent vessel at the aneurysm ostium. In conjunction with the increasing use of self-expanding intracranial microstents, we designed a second-generation device, a V-POD (made of nitinol), and tested this device in an elastase-induced rabbit aneurysm model. Our intent was to improve the previous stent design and to determine the feasibility of deploying these devices and whether this device could achieve adequate flow diversion and aneurysm healing.

Materials and Methods

Stent Designs and Platform

Three V-POD types were used in this study: Type A was made by adding a low-porosity section (patch) around the entire device circumference on a closed-cell design platform (Fig 1*A*); type B had the patch covering only a partial device circumference on a closed-cell platform (Fig 1*B*); and type C, which was used only in a few cases, was similar to type B but on an open-cell platform (Fig 1*C*). The type A stent required placement precision only in the transverse direction relative to the aneurysm orifice and needed 2 platinum radiopaque markers for precise localization of the low-porosity region. Types B and C required placement precision in the transversal and azimuthal directions; localization of the low-porosity patch can be achieved by using a set of 4 markers arranged in a quadrature.[13] Type A was designed for aneurysms without perforators in the immediate circumference of the aneurysm-bearing parent vessel; types B and C were designed for aneurysms with perforators in that same region.

The devices were designed, by using AutoCAD software (Autodesk, http://usa.autodesk.com), to be similar to current commercially available intracranial self-expanding microstents. They were cut in a laser machine shop (Laserage, Waukegan, Illinois) by using nitinol tubing (Ni-Ti Tubes, http://www.ni-ti.com/about.shtml) with 100-μm wall thickness. After the devices were machined, they were heat-shaped to a 4-mm expanded diameter and then electropolished by using commercially available chemicals (RD-Chemical, http://rdchem.com).

The electropolished devices were coated by using a polymer, poly($MPC_{0.3}$-co-$BMA_{0.7}$) (NOF Corp, Tokyo, Japan)[14] to decrease the chance of in-stent restenosis and friction between the stent and catheter during delivery. Finally, hydrophilic, 0.45-μm pore size, 80% porous, and 65-μm thick PTFE patches (Millipore, http://www.millipore.com) were attached onto the stents by using ChronoFlex AR polyurethane (AdvanSource Biomaterials, Wilmington, Massachusetts).

Aneurysm Creation and Stent Placement

Procedures were approved by the Animal Care and Use Committee at the authors' institution and were conducted according to Animal Welfare Act guidelines. Twenty New Zealand white rabbits (mean weight, 3.2 $\pm$ 0.75 kg; range, 3–3.5 kg) underwent right carotid artery elastase model aneurysm creation.[15] The aneurysms were treated 3 weeks later. After treatment, the rabbits were placed on antiplatelet medication (aspirin, 5 mg per kg per day). Follow-up angiography was performed 4 weeks' posttreatment, after which the aneurysms were explanted.

The femoral artery was accessed after a cut-down with a 5F introducer sheath. With road-mapping, a high-support 0.014-inch Choice-PT guidewire (Boston Scientific, Natick, Massachusetts) was advanced to the subclavian artery. A preloaded catheter (partially visible in Fig 1) containing the V-POD was advanced to the aneurysm location. At the beginning of the study, we used 5F stent catheters. As we improved our stent and delivery design, we were able to use smaller 3.5F catheters. A high-resolution roadmap was acquired with a region-of-interest microangiographic detector to facilitate precise stent placement.[13,16] This detector has a 4-cm FOV with 35-μm pixels, is attached onto the angiographic C-arm, and is used whenever high resolution is needed over a small region of interest. The stent-containing catheter was advanced over the aneurysm ostium by using the markers on the patch as references. Under roadmap, the catheter position was adjusted until the patch faced the aneurysm orifice.

For type A stents, the catheter was adjusted such that the 2 markers indicated by the 2 solid black arrows in Fig 1 spanned the aneurysm ostium entirely; the azimuthal position was not important. For types B and C, the catheter was positioned such that proximal and distal platinum markers were adjacent to and spanned the entire aneurysm ostium, while the middle platinum markers were overlapping or placed at the same distance from the aneurysm orifice. If the imaging plane was not quite parallel to the catheter, the middle markers were slightly separated axially; however, if the lateral distance to the aneurysm ostium was the same, the patch faced the orifice. The azimuthal position was adjusted by rotating the microcatheter containing the stent. After each slight rotation, the catheter was moved slightly back and forth to release strain due to friction. A stent pusher was then advanced against the stent; the outer stent-containing catheter was pulled back until the stent was unsheathed.

The initial study plan was to successfully treat 20 elastase aneurysms with different asymmetric stents, approximately equally distributed between asymmetric and circumferential types. At the time of the investigation, there were 2 stents (open- and closed-cell) of each kind (asymmetric and circumferential); the interventionists could choose any of these. Initially, open-cell circumferential stents (type C) were used, but interventionists soon opted for a closed-cell design (stent types A and B), which was much easier to deploy in comparison with the open-cell design.

Angiographic Data Analysis

Changes in CA flow in the aneurysm dome before and immediately after stent placement were assessed via angiography by tracking the amount of CA entering the dome. The maximum CA amount entering the aneurysm dome was normalized to the CA-measured bolus passing through the parent vessel[17] to eliminate variation due to injection parameters. Both pre- and poststent normalized maximum CA values were measured as percentages of the total bolus injected, and an immediate poststent/prestent ratio was calculated. The ratio is a direct measure of flow reduction in the aneurysm sac after device

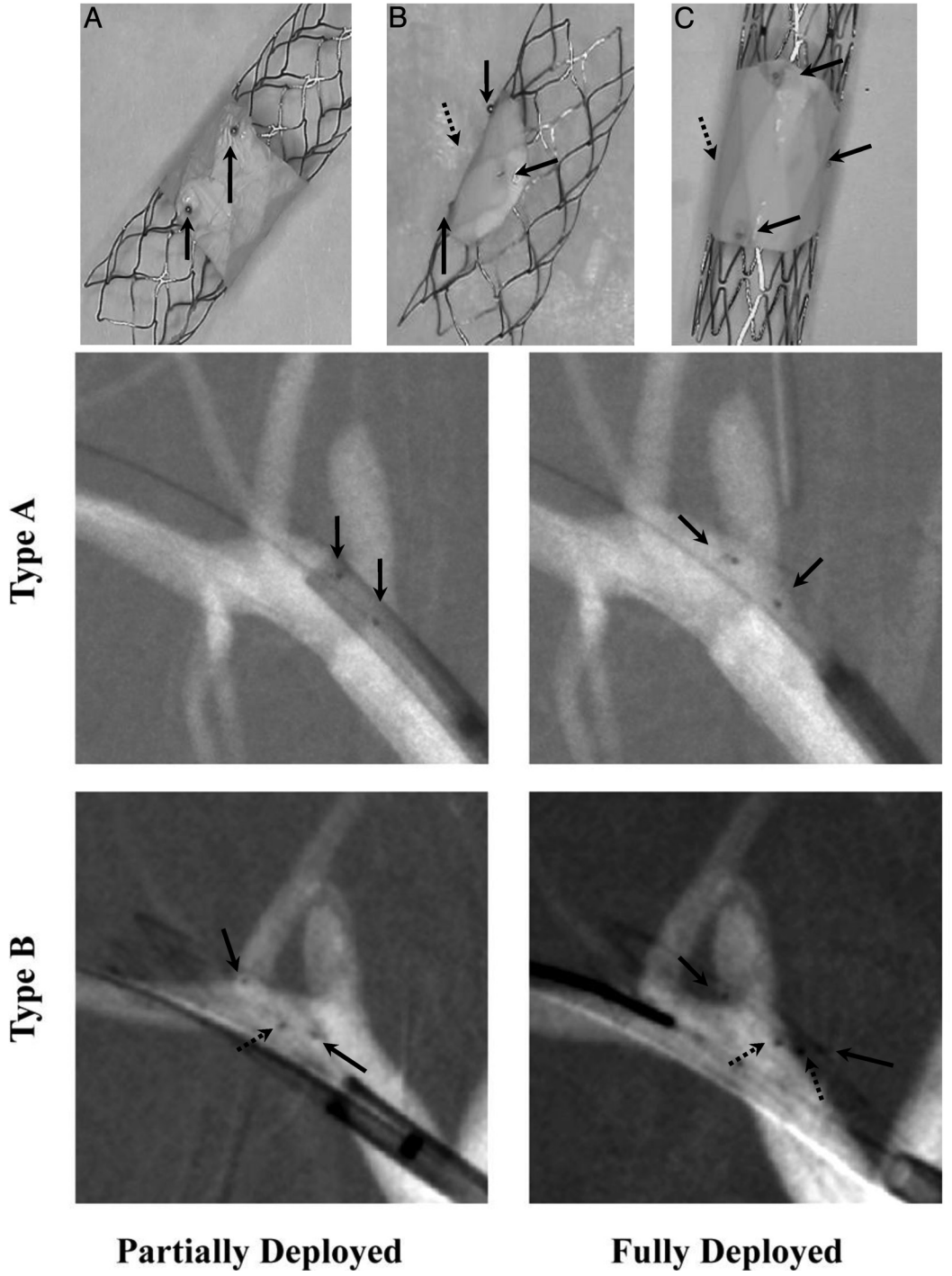

Fig 1. *A–C,* Self-expanding V-POD devices. Upper: Photographs of the 3 types of these stents. Lower: Angiograms showing deployment of types A and B. Type A contains a sleeve (PTFE patch) approximately 4–5 mm wide covering the central part of the stent; types B and C have a patch covering only a given stent region. Types A and B have a closed-cell structure, whereas type C has an open-cell structure. In the photographs, black arrows indicate the platinum markers used to guide the stents during the procedure and dotted arrows indicate the marker position not visible in photographs. Modified with permission from Ionita et al.[17]

deployment. On the basis of previous reports,[5,18] flow diversion was considered successful when the maximum CA immediate poststent/prestent ratio was <1.

CA flow measurement in angiograms is severely affected by variations such as catheter position, x-ray parameters, and body position. These parameters generally do not change between prestenting and immediate poststenting angiograms, at least with imaging of this aneurysm model, but they may change at 4 weeks' follow-up. Thus, instead of measuring CA flow at 4 weeks, we graded the follow-up angiograms on the basis of the aneurysm filling with contrast compared with the prestenting angiographic run by using the following scale: 0) aneurysm was completely filled; 1) <0.75; 2) <0.50; 3) <0.25; 4) no filling but exhibiting some remnant neck; and 5) no CA flow in the aneurysm dome or neck (total occlusion).

The degree of occlusion was graded independently by 2 authors (C.N.I., S.K.N.). Because of the possible variability in differentiating

angiographic aneurysm occlusion, if there was a discrepancy between grades assigned by the 2 observers, they discussed the issue and a third observer (S.R.) assigned the final occlusion category.

Conebeam Micro-CT Analysis

At 4 weeks' follow-up, aneurysms were fixed by pressure perfusion; then they were explanted and stored by using a solution of 2.5% glutaraldehyde and 2% of 0.9 neutral-buffered formalin in 0.1 mol/L of sodium cacodylate (Polysciences, Warrington, Pennsylvania). Aneurysm samples were dissected, and tissue was removed down to the arterial wall under microscopic visualization and connected to an air-flow circuit for 1–2 minutes to replace the fixation solution with air for better CA visualization during conebeam micro-CT scanning.[19] The 3D volume obtained from the micro-CT data was then imported into a Vitrea Workstation (Vital Images, Minnetonka, Minnesota), and the thrombosed volume relative to the total aneurysm dome volume was calculated.

An operator examined every fourth section of the CT scan on the axial and transverse images (with respect to the aneurysm dome) and outlined manually first the aneurysm dome sample and then the nonthrombosed volume. The dome included the vessel wall starting from the ostium of the parent artery to the apex of the aneurysm and thus included the entire aneurysm (dome and neck). The percentage of the total aneurysm volume occlusion was further calculated. Despite the high micro-CT resolution (45 μm), there was an error associated with the manual selection of a boundary; hence, we refer to this measurement as an approximation.

Histologic Analysis

Aneurysms were excised along with the parent vessel, processed, embedded in paraffin, and cut into 2-μm-thick sections taken from the aneurysm midpoint in the coronal orientation (same direction as the parent artery) by using a rotary microtome (HM355S; Microm International, Walldorf, Germany). Slides were stained with Masson trichrome to determine the collagen deposition. A grading scale recommended by Dai et al[20] was used to evaluate the presence of organized thrombus in the aneurysm dome and neck area: 0) fresh blood clot or no thrombus, 1) organized thrombus in less than one-third of the area, 2) organized thrombus in one-third to two-thirds of the area, 3) organized thrombus in more than two-thirds of the area, 4) completely organized loose thrombus, and 5) completely organized attenuated fibrous tissue.

SEM

SEM was performed on all stented-artery specimens: The arterial trunk was longitudinally cut opposite the aneurysm ostium. The stented vessel walls were opened and dehydrated in ethanol (70%–100%), and then they were dried with hexamethyldisilazane (Polysciences). Parent vessel SEM was performed for an "in-vessel" surface view, by using a field-emission scanning electron microscope (Hitachi 9000, Pleasanton, California). Endothelialization was evaluated at stent ends and over the PTFE patch. A 0–3 scale was assigned to quantify the degree of endothelialization: 0) no cell coverage; 1) partial coverage with ECM and endothelial cells, 2) full coverage with ECM and endothelial cells, and 3) full coverage with endothelial cells.

Statistical Analysis

The total number of treated aneurysms and the division into separate groups were selected to be similar to those in previous publications[3,6,21] to maximize resources while providing acceptable statistical power. Data are presented as mean ± SD (range) for continuous variables such as pre- and poststent normalized maximum CA and total aneurysm volume and as median and frequency for ordinal variables such as follow-up grade, histology, and SEM grades. Statistical analysis was performed by using InStat (GraphPad Software, La Jolla, California). The Spearman correlation coefficient and Student *t* test assuming equal variances were used to determine statistical significance or correlation among different parameters (eg, aneurysm geometry, angiographic measurements, and conebeam micro-CT and stented-artery specimen histology). The Fisher exact test was used for 2-stent group comparison (A versus B and C). Significance was defined as $P < .05$.

Results

Procedural Results

Geometries and parent vessel diameter measurements of the created aneurysms were 2.5 ± 0.6 mm (range, 1.9–3.1 mm) for the parent vessel, 2.4 ± 0.9 mm (range, 1.6–5.1 mm) for the aneurysm ostium, 4.7 ± 2.1 mm (range, 2.4–11.4 mm) for the aneurysm dome, and 2.0 ± 0.4 (range, 1.2–2.7) for the dome-to-ostium ratio. Type A stents were used in 9 aneurysms; type B, in 7; and type C, in 4. A comparison of group-wise aneurysm geometry measurements by using the Student *t* test yielded a *P* value $> .05$, indicating no significant correlation among the 3 groups of stents.

The type A stent required approximately 1 minute to align and deploy, once the stent was brought to the aneurysm location. Types B and C required between 3 and 5 minutes to align and deploy. The most challenging part of the deployment was roadmap mismatching with the anatomic structures due to the location of the aneurysm in an area surrounded mostly by soft tissue. During alignment and deployment, the interventionists injected a small amount of contrast material to verify the aneurysm location.

Mechanical delivery problems were encountered in 4 of 20 aneurysms (1 type A stent and 3 type B). The single type A stent failure was due to incomplete stent expansion that was not observed at the time of deployment and caused partial vessel occlusion. The 3 delivery problems with type B stents were most probably due to excessive electropolishing and radial stent-force weakening, which, in turn, caused stent migration immediately postdelivery. This was seen earlier in this experience and was corrected in subsequent cases. Our result analysis excludes the 4 mechanical failures. No vessel injury was encountered during the entire experiment, unlike with previous balloon-mounted AVS designs,[4] in which vessel injury occurred in 3 of 13 stent-treated aneurysms.

Angiographic Results

Figure 2 shows examples of angiograms of treated aneurysms. Tables 1 and 2 give a summary of the main results, including CA filling before and after treatment. Before treatment, the maximum CA amount measured in the aneurysms accounted for 3.07 ± 2.14% (range, 0.24%–8.4%) of the total bolus passing through the parent vessels. After stent placement, this decreased to 0.44 ± 0.86% (range, 0.0%–2.72%), with 9 aneurysms showing negligible or no CA entering the aneurysm. Flow reduction, measured in terms of immediate poststent/prestent maximum CA en-

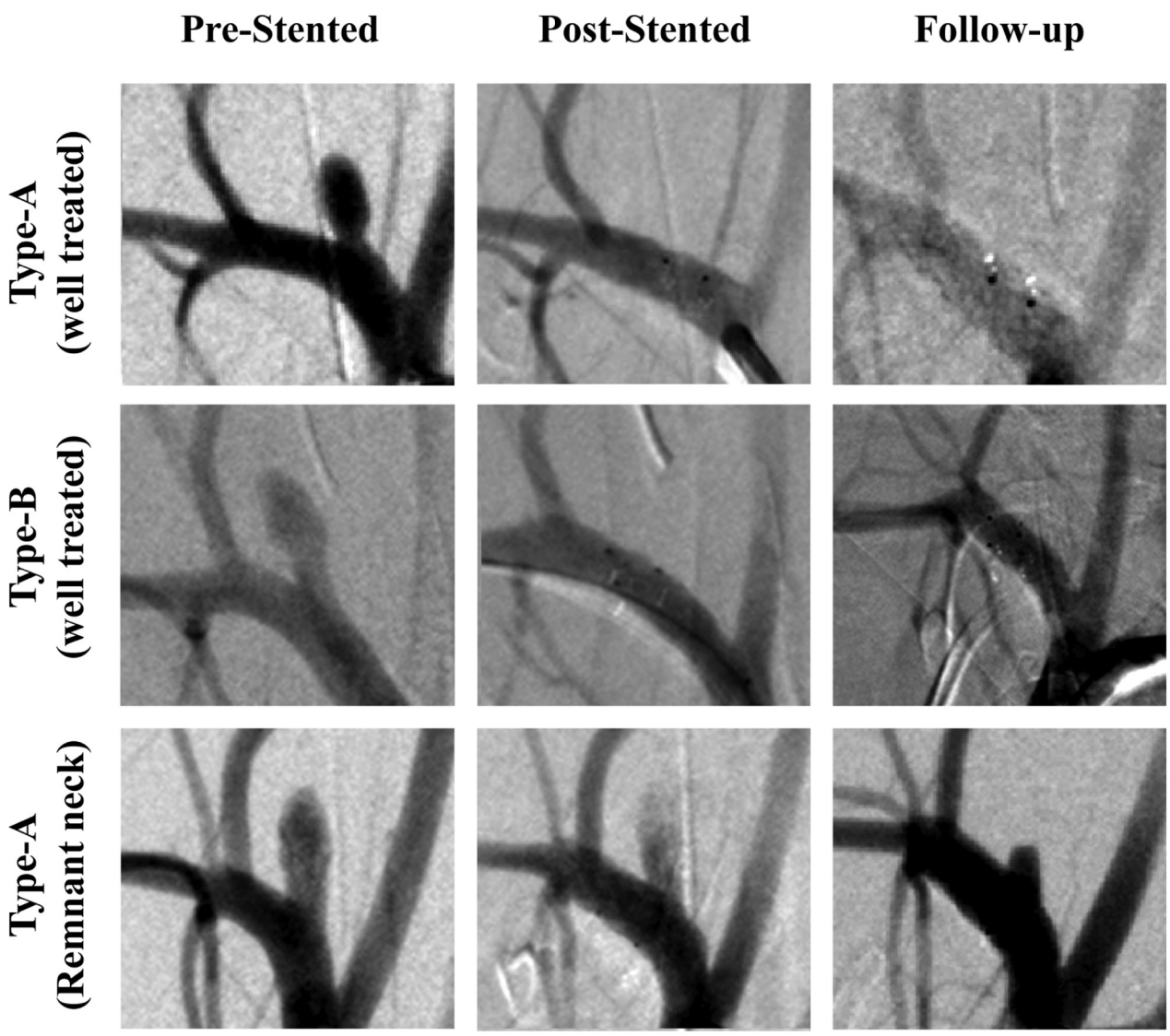

Fig 2. Angiograms of aneurysms treated with V-POD. Column headings indicate angiogram acquisition time (prestenting, immediately poststenting, and 4 weeks later). First row, an aneurysm treated with V-POD-A; second row, aneurysm treated with V-POD-B; third row, aneurysm treated with V-POD-A showing a remnant neck.

tering the aneurysm, was 0.13 ± 0.18 (range, 0.0–0.5). The 4-week posttreatment angiography runs indicated no aneurysm filling in 10 of 16 (63%) treated aneurysms (follow-up grade 5), 3 of 16 (~19%) with no aneurysm filling but exhibiting a small remnant neck (follow-up grade 4), and 3 of 16 (~19%) with <0.25 filling (follow-up grade 3). Angiographic results for type A versus types B and C were compared by using the Student *t* test; this comparison yielded a $P > .05$, showing no significant correlation between the type of stent used and CA flow reduction after stent placement. The Spearman correlation factor for immediate poststent/prestent peak ratios and follow-up angiographic results was 0.67 with $P = .005$.

Conebeam Micro-CT Results

The total aneurysm occlusion percentage (ie, the average of the approximate volume occupied by thrombus in each aneurysm), measured by using the micro-CT scanner, was, on average, 96 ± 6.8% (range, 80%–100%), with 11 aneurysms showing complete occlusion; 3 aneurysms with remnant necks (nonthrombosed volume <11% of total aneurysm dome); and 2 aneurysms, though not fully thrombosed, demonstrating >80% occlusion (80%–82%). Representative sample micro-CT sections are shown in Fig 3. The Fisher exact test comparing occluded versus partially occluded aneurysms in the 2 stent groups (A versus B and C) yielded $P = .608$ (not significant).

Ostium-coverage estimation by using micro-CT could only be evaluated from the position of the markers relative to the aneurysm ostium. In all 16 aneurysms in which V-PODs were successfully deployed, the patch was placed accurately, covering 100% of the aneurysm orifice. Comparison with a previous study reporting balloon-deployable AVS data[4] revealed no significant difference in total aneurysm occlusion rates; however, stent placement during the x-ray–guided procedure was more accurate for the V-POD (16/16) versus the AVS (4/9) ($P = .032$). We excluded the 4 stents that had mechanical delivery/expansion problems, because these occurred postdelivery and were not related

Table 1: Results for successful deployment[a]

	Angiograms				Micro-CT	Histology Grade		SEM Grade	
Case	Prestent	Poststent	Post/Pre Ratio	Follow-Up Grade	Total Aneurysm Occlusion (%)	Dome[b]	Neck	Stent Struts	Patch
1-A	2.21	0.59	0.27	5	100	5	5	3	3
2-A	4.32	0	0.00	5	100	3	5	3	0
4-A	3.42	0	0.00	5	100	4	5	3	2
5-A	0.89	0	0.00	5	100	2	5	3	1
6-A	5.49	2.72	0.50	4	89	5	0	3	2
7-A	1.85	0.24	0.13	3	82	3	0	3	3
8-A	2.5	0	0.00	5	100	4	3	3	2
9-A	0.24	0.02	0.08	5	100	4	5	3	3
10-B	0.4	0	0.00	4	95	4	0	3	2
11-B	3.2	0	0.00	5	100	2	5	3	3
14-B	4.6	0	0.00	5	100	4	5	3	2
16-B	1.83	0.55	0.30	3	80	5	0	3	2
17-C	2.7	0	0.00	5	100	1	5	3	1
18-C	1.83	0.55	0.30	3	100	5	0	3	2
19-C	5.25	2.4	0.46	4	92	5	0	3	2
20-C	8.4	0.02	0.02	5	100	5	5	3	3
Average (Median)	3.07 ± 2.14	0.44 ± 0.86	0.13 ± 0.18	5	96 ± 6.8	4	5	3	2

[a] Columns 2 and 3, maximum percentage of total injected contrast material entering the aneurysm dome pre- and immediately poststent; 4, immediate poststent/prestent ratios of maximum CA volume entering the aneurysm dome; 5, follow-up angiographic grades: 0) intact aneurysm, 1) 0.75–0.50 filling, 2) 0.50–0.25 filling, 3) <0.25 filling, 4) no filling but exhibiting some remnant neck, 5) no CA flow in the aneurysm dome or neck (total occlusion); 6, conebeam micro-CT scanning result—thrombosed volume relative to total aneurysm dome volume (%)—total aneurysm occlusion; 7 and 8, histology grade for dome and neck[20]: 0) fresh blood clot or no thrombus, 1) organized thrombus in less than one-third of the area, 2) organized thrombus in one-third to two-thirds of the area, 3) organized thrombus in more than two-thirds of the area, 4) completely organized loose thrombus, 5) completely organized dense fibrous thrombus; 9 and 10, SEM grade for degree of endothelialization of stent and patch: 0) no cell coverage, 1) partial coverage with ECM and endothelial cells, 2) full coverage with ECM and endothelial cells, 3) full coverage with endothelial cells.
[b] Histology grade for the partially thrombosed aneurysm dome and refers to the thrombosed portion of the dome.

Table 2: Results for stents with mechanical failures[a]

	Angiograms			Micro-CT		Histology Grade		SEM Grade	
Case	Prestent	Poststent	Post/Pre Ratio	Follow-Up Grade	Total Aneurysm Occlusion (%)	Dome[b]	Neck	Stent Struts	Patch
3-A	0.68	3.14	4.62	2	55	4	0	1	1
12-B	3.44	0.33	0.10	3	60	4	0	3	2
13-B	1.53	2.70	1.76	2	20	0	0	3	3
15-B	1.82	0.69	0.38	3	30	3	0	3	2
Average	2.83 ± 2.02	0.69 ± 1.1	0.45 ± 1.06	4.5	85 ± 25	4	1.5	3	2

[a] Columns 2 and 3, maximum percentage of total injected contrast material entering the aneurysm dome pre- and immediately poststent; 4, immediate poststent/prestent ratios of maximum CA volume entering the aneurysm dome; 5, follow-up angiographic grades: 0) intact aneurysm, 1) 0.75–0.50 filling, 2) 0.50–0.25 filling, 3) <0.25 filling, 4) no filling but exhibiting some remnant neck, 5) no CA flow in the aneurysm dome or neck (total occlusion); 6, conebeam micro-CT scanning result—thrombosed volume relative to total aneurysm dome volume (%)—total aneurysm occlusion; 7 and 8, histology grade for dome and neck[20]: 0) fresh blood clot or no thrombus, 1) organized thrombus in less than one-third of the area, 2) organized thrombus in one-third to two-thirds of the area, 3) organized thrombus in more than two-thirds of the area, 4) completely organized loose thrombus, 5) completely organized dense fibrous thrombus; 9 and 10, SEM grade for degree of endothelialization of stent and patch: 0) no cell coverage, 1) partial coverage with ECM and endothelial cells, 2) full coverage with ECM and endothelial cells, 3) full coverage with endothelial cells.
[b] Histology grade for the partially thrombosed aneurysm dome and refers to the thrombosed portion of the dome.

directly to the deployment procedure. In the previous study, misplacement occurred due to infolding of the balloon, which caused the stent to rotate slightly during the deployment.

Histology and SEM Results

The median dome histology grade was 4 (range, 1–5); representative sections and grading are shown in Fig 4. Most occluded areas showed intermediate healing processes characterized by organized loose tissue. Six of 16 (38%) aneurysm domes displayed completely organized attenuated fibrous tissue; 5/16 (~31%), completely organized loose thrombus; 2/16 (~13%), organized thrombus in more than two-thirds of the area; 2/16 (~13%), organized thrombus in one-third to two-thirds of the area; and 1/16 (~6%), organized thrombus in less than one-third of the area. The median aneurysm neck histology grade was 5 (range, 0–5). The neck histology grading distribution was as follows: 9/16 (~56%) displayed completely organized attenuated fibrous tissue; 1/16 (~6%), organized thrombus in more than two-thirds of the area; and 6/16 (~38%), fresh blood clot or no thrombus. The average correlation between the immediate poststent/prestent ratio and the follow-up angiogram, micro-CT scan, and histology scores was $r = 0.60$, with a $P < .05$.

SEM results showed complete endothelialization of the stent struts at the edges in 16/16 (100%) cases. Endothelialization samples and grading are shown in Fig 5. In 5/16 (~31%) cases, the patch was fully covered with endothelial cells; in 8/16 (50%), it was fully covered with ECM and endothelial cells; in 2/16 (~13%), it was partially covered with ECM and endothelial cells; and in 1/16(~6%), no cell growth was observed on the patch.

Discussion

In this study, we describe the design, feasibility, and effectiveness of a new V-POD intended for IA occlusion in a rabbit elastase aneurysm model. Compared with previous designs of AVS,[4,5] the new stent is easier to maneuver and deploy. We did

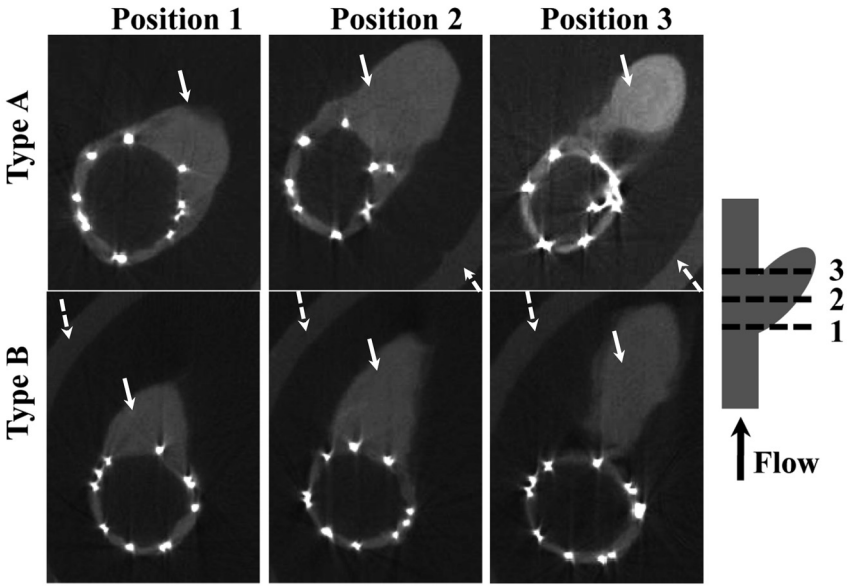

Fig 3. Micro-CT sections of explanted aneurysms treated with 2 types of V-POD taken at 3 positions, as indicated in the schematic. Brighter dots are the nitinol struts of the stents, white arrows indicate the soft tissue, and dotted arrows indicate the holder. The PTFE patch is not visible because it has an attenuation similar to that of the soft tissue. The artery lumen is filled with air, and the intensity value is the same as that outside the sample. There are no cavities filled with air in the aneurysm dome, indicating total aneurysm occlusion.

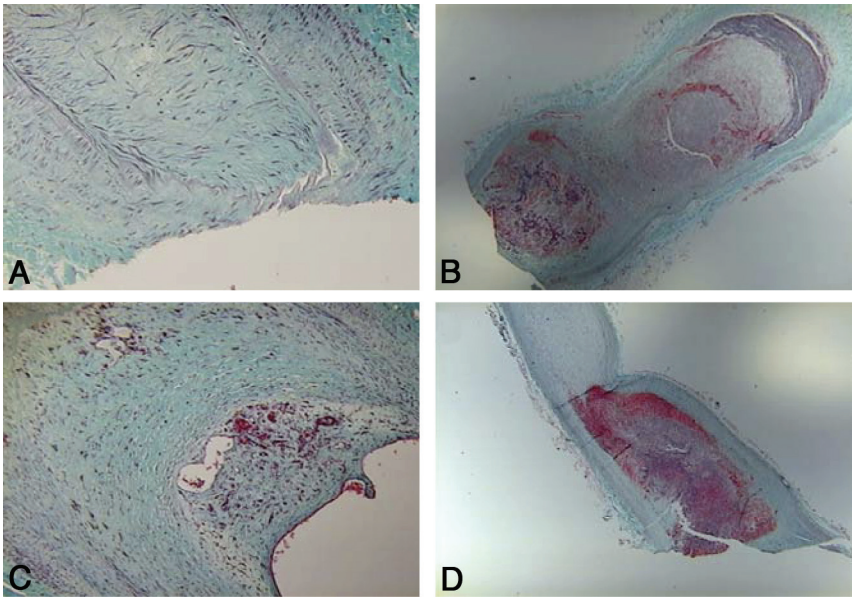

Fig 4. Histology samples stained with Masson trichrome. *A*, Grade 5 aneurysm (completely organized attenuated fibrous tissue) (original magnification, ×40). *B*, Grade 2 result for organized tissue in one-third to two-thirds of the dome area (original magnification, ×5). *C*, Grade 5 for the aneurysm dome and grade 0 for the neck area (original magnification, ×10). *D*, Grade 1 for organized tissue in less than one-third of the dome area (original magnification, ×5).

not experience any vessel injury, as previously reported by using AVS. At the beginning of the study, stents were placed by using a 5F straight catheter. As our capability to attach the patch and electropolish the stents to a smaller strut diameter increased, we were able to load the stent into a 3.5F catheter. Open-cell type C V-PODs were more difficult to navigate than closed-cell designs A and B, and the closed-cell platform became the preferred design for the V-POD. The patch material was chosen on the basis of biocompatibility[22-24] and mechanical properties. We used the thinnest medical-grade PTFE patch available from laboratory suppliers. However, different materials can be used, as long as they are attenuated enough to cause sufficient redirection of flow away from the aneurysm ostium. Our results of 96% total aneurysm occlusion on average (derived from 3D-volume micro-CT scanning data) with 20% showing some remnant neck at only 4 weeks of follow-up are comparable with previous results[4] in which 100% occlusion of 9 treated aneurysms was reported. The lower rate of total aneurysm occlusion in the present study, by comparison with the previously reported result[4] of 100% occlusion, may be related to the PTFE material used in this study. This very thin material might have oscillated with the pulsatile flow in the ostium region, thus delaying cell proliferation. In the present cases, no significant neointimal hyperplasia was observed. The correlation between angiographic results and treatment outcome was quite significant.

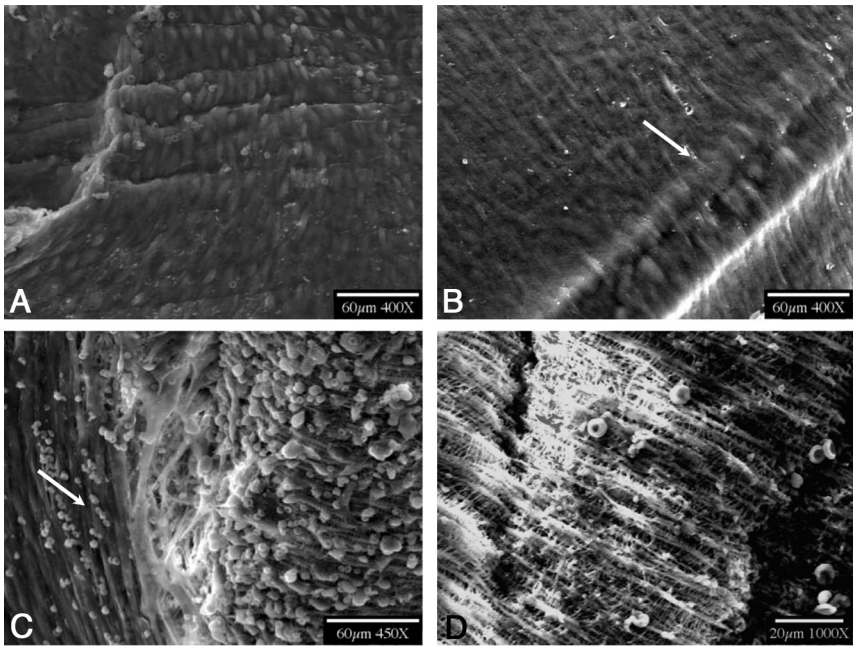

Fig 5. SEM photographs. *A*, Fully covered asymmetric patch (SEM, grade 3). *B*, Strut covered by endothelial cells (SEM, grade 3). *C*, PTFE patch of a stent partially covered with endothelial cells (*arrow*) and partially with ECM (SEM, grade 1). *D*, PTFE patch totally exposed with no tissue adherent to the surface (SEM, grade 0).

Both device designs (circumferential patch [type A] and focal/asymmetric patch [types B and C]) offer the possibility of treating aneurysms when branches or perforators are located in stent areas with high porosity. Type B V-POD placement took longer and required increased fluoroscopy time due to difficult stent delivery to the desired site.

IA occlusion and preservation of nearby perforators and branch vessels are closely associated treatment goals and cannot be ignored when designing a flow-diversion device. Unfortunately, to our knowledge, animal models in which both concerns (aneurysm occlusion and perforator preservation) can be addressed are virtually nonexistent. In the aneurysm animal model used in this study, the ability of the new devices to preserve branch vessels could not evaluated. We have verified only the first aspect (aneurysm occlusion). However, we can speculate that the V-POD has a higher chance of achieving flow diversion with a lower likelihood of perforator or branch vessel occlusion, because the design of this stent has a very high-porosity structure everywhere except at the aneurysm ostium; in fact, the design outside the patch is similar to intracranial self-expanding microstents currently used safely in several clinical applications. We posit that branch vessels and perforators could be preserved, unless they are close to the aneurysm ostium and covered by the patch itself. For these specific cases, we envision patient-specific V-PODs that could be rapidly engineered, fabricated, and tailored to the specific aneurysm ostium and parent-vessel configuration of an individual patient.[25]

Type A stent placement presented no design or deployment issues and resulted in good aneurysm occlusion. However, for stent types B and C, catheter-delivery issues and stent-design issues that preserve the radial expansive force are currently being improved. These issues appear to be mostly related to rotational catheter actuation in a remote area. Our study demonstrated that accurate deployment is possible but may at times be difficult.

The main limitations of this study are the small number of aneurysms in which the V-POD was tested and the translatability of results in a rabbit aneurysm model to those in an IA in a patient.[15] Although it is intuitive that this device would be able to better preserve branch vessels and perforators, further testing is required. Nevertheless, the V-POD achieved good flow diversion and aneurysm healing when deployed properly. We are currently working on and have improved the deployment mechanisms in the type B stents. We believe that V-POD-like flow-diversion devices will be increasingly applied for IA treatment in the clinical setting.

Conclusions

This report demonstrates the feasibility and effectiveness of the V-POD for aneurysm occlusion in a rabbit elastase aneurysm model. When properly deployed, this device has been shown to be deliverable and to achieve definitive treatment and total thrombosis in 69% of the aneurysms and to induce >80% thrombosis in the remaining aneurysms.

Acknowledgments

We thank Robert E. Baier, PhD, Peter J. Bush, MSc, Liza C. Pope, BSc, Andrey Sinelnikov, BS, and Hajime Ohta, MD PhD, for their collaboration, and Paul H. Dressel, BFA, for assistance with preparation of the illustrations.

Disclosures: Dr Bednarek receives research support from NIH grants R01NS43924 and R01EB002873 and equipment from Toshiba Medical Systems Corporation. Dr Hopkins receives research support from Toshiba; serves as a consultant to Abbott, Boston Scientific, Cordis, Micrus, and W.L. Gore; holds a financial interest in AccessClosure, Boston Scientific, Claret Medical Inc., Micrus, and Valor Medical; has a board/trustee/officer position with AccessClosure, Claret Medical Inc., and, until September of 2010, with Micrus; belongs to the Abbott Vascular speakers' bureau; and receives honoraria from Bard, Boston Scientific, Cordis, Memorial Healthcare System, Complete Conference Management, The Society for Cardiovascular Angiography and Interventions (SCAI), and the Cleveland Clinic. Dr Ionita receives research support from NIH grants R01NS43924 and R01EB002873. Dr Levy receives research grant support (principal investigator: Stent-Assisted Recanalization in Acute Ischemic Stroke), other research support (devices), and

honoraria from Boston Scientific and research support from Codman & Shurtleff Inc and ev3/Covidien Vascular Therapies; has ownership interests in Intratech Medical Ltd and Mynx/AccessClosure; serves as a consultant on the board of scientific advisors to Codman & Shurtleff Inc; serves as a consultant per project and/or per hour for Codman & Shurtleff Inc, ev3/Covidien Vascular Therapies, and TheraSyn Sensors Inc; and receives fees for carotid stent training from Abbott Vascular and ev3/Covidien Vascular Therapies. Dr Levy receives no consulting salary arrangements. All consulting is per project and/or per hour. Dr Natarajan is the recipient of the 2010–2011 Cushing Award of the Congress of Neurological Surgeons. Dr Rudin receives research support from NIH grants R01NS43924 and R01EB002873 (principal investigator) and equipment from Toshiba Corporation. Dr Siddiqui has received research grants from the NIH (coinvestigator: National Institute of Neurological Disorders and Stroke 1R01NS064592–01A1, Hemodynamic Induction of Pathologic Remodeling Leading to Intracranial Aneurysms) and the University at Buffalo (Research Development Award); holds financial interests in Hotspur, Intratech Medical, StimSox, and Valor Medical; serves as a consultant to Codman & Shurtleff Inc, Concentric Medical, ev3/Covidien Vascular Therapies, GuidePoint Global Consulting, and Penumbra; belongs to the Speakers' Bureaus of Codman & Shurtleff Inc and Genentech; serves on an advisory board for Codman & Shurtleff Inc; and has received honoraria from the American Association of Neurological Surgeons courses, an Emergency Medicine Conference, Genentech, Neocure Group LLC, and from Abbott Vascular and Codman & Shurtleff Inc for training other neurointerventionists in carotid stenting and for training physicians in endovascular stenting for aneurysms. Dr Siddiqui receives no consulting salary arrangements. All consulting is per project and/or per hour. Mr Wang receives research support from NIH grants R01NS43924 and R01EB002873.

References

1. Canton G, Levy DI, Lasheras JC, et al. **Flow changes caused by the sequential placement of stents across the neck of sidewall cerebral aneurysms.** *J Neurosurg* 2005;103:891–902
2. Fiorella D, Albuquerque FC, Deshmukh VR, et al. **Endovascular reconstruction with the Neuroform stent as monotherapy for the treatment of uncoilable intradural pseudoaneurysms.** *Neurosurgery* 2006;59:291–300, discussion 291–300
3. Kallmes DF, Ding YH, Dai D, et al. **A new endoluminal, flow-disrupting device for treatment of saccular aneurysms.** *Stroke* 2007;38:2346–52
4. Ionita CN, Paciorek AM, Dohatcu A, et al. **The asymmetric vascular stent: efficacy in a rabbit aneurysm model.** *Stroke* 2009;40:959–65
5. Ionita CN, Paciorek AM, Hoffmann KR, et al. **Asymmetric vascular stent: feasibility study of a new low-porosity patch-containing stent.** *Stroke* 2008;39:2105–13
6. Kallmes DF, Ding YH, Dai D, et al. **A second-generation, endoluminal, flow-disrupting device for treatment of saccular aneurysms.** *AJNR Am J Neuroradiol* 2009;30:1153–58
7. Kallmes DF, Comstock BA, Heagerty PJ, et al. **A randomized trial of vertebroplasty for osteoporotic spinal fractures.** *N Engl J Med* 2009;361:569–79
8. van Rooij WJ, Sluzewski M. **Perforator infarction after placement of a Pipeline flow-diverting stent for an unruptured A1 aneurysm.** *AJNR Am J Neuroradiol* 2010;31:E41–43. Epub 2010 Feb 11
9. Kulcsar Z, Ernemann U, Wetzel SG, et al. **High-profile flow diverter (SILK) implantation in the basilar artery: efficacy in the treatment of aneurysms and the role of the perforators.** *Stroke* 41:1690–96
10. Lylyk P, Miranda C, Ceratto R, et al. **Curative endovascular reconstruction of cerebral aneurysms with the Pipeline embolization device: the Buenos Aires experience.** *Neurosurgery* 2009;64:632–43
11. Szikora I, Berentei Z, Kulcsar Z, et al. **Treatment of intracranial aneurysms by functional reconstruction of the parent artery: the Budapest experience with the Pipeline embolization device.** *AJNR Am J Neuroradiol* 2010;31:1139–47. Epub 2010 Feb 11
12. Turowski B, Macht S, Kulcsar Z, et al. **Early fatal hemorrhage after endovascular cerebral aneurysm treatment with a flow diverter (SILK-Stent): do we need to rethink our concepts?** *Neuroradiology* 2011;53:37–41. Epub 2010 Mar 26
13. Ionita CN, Rudin S, Hoffmann KR, et al. **Microangiographic image-guided localization of a new asymmetric stent for treatment of cerebral aneurysms.** *Proc Soc Photo Opt Instrum Eng* 2005;5744:354–65
14. Nakabayashi N, Williams DF. **Preparation of non-thrombogenic materials using 2-methacryloyloxyethyl phosphorylcholine.** *Biomaterials* 2003;24:2431–35
15. Altes TA, Cloft HJ, Short JG, et al. **1999 ARRS Executive Council Award: creation of saccular aneurysms in the rabbit—a model suitable for testing endovascular devices. American Roentgen Ray Society.** *AJR Am J Roentgenol.* 2000;174:349–54
16. Ionita CN, Keleshis C, Patel V, et al. **Implementation of a high-sensitivity micro-angiographic fluoroscope (HS-MAF) for in-vivo endovascular image guided interventions (EIGI) and region-of-interest computed tomography (ROI-CT).** *Proc Soc Photo Opt Instrum Eng* 2008;6918:69181I
17. Ionita CN, Wang W, Bednarek DR, et al. **Assessment of contrast flow modification in aneurysms treated with closed-cell, self-expanding asymmetric vascular stents (SAVS).** *Proc Soc Photo Opt Instrum Eng* 2010;7626:76260I
18. Sadasivan C, Cesar L, Seong J, et al. **Treatment of rabbit elastase-induced aneurysm models by flow diverters: development of quantifiable indexes of device performance using digital subtraction angiography.** *IEEE Trans Med Imaging* 2009;28:1117–25
19. Ionita CN, Hoffmann KR, Bednarek DR, et al. **Cone-beam micro-CT system based on LabVIEW software.** *J Digit Imaging* 2008;21:296–305. Epub 2008 Apr 24
20. Dai D, Ding YH, Lewis DA, et al. **A proposed ordinal scale for grading histology in elastase-induced, saccular aneurysms.** *AJNR Am J Neuroradiol* 2006;27:132–38
21. Sadasivan C, Cesar L, Seong J et al. **An original flow diversion device for the treatment of intracranial aneurysms: evaluation in the rabbit elastase-induced model.** *Stroke* 2009;40:952–58
22. Jamshidi P, Mahmoody K, Erne P. **Covered stents: a review.** *Int J Cardiol* 2008;130:310–18. Epub 2008 Jul 30
23. Störger H, Haase J. **Polytetrafluoroethylene-covered stents: indications, advantages, and limitations.** *J Interv Cardiol* 1999;12:451–56
24. Burbelko MA, Dzyak LA, Zorin NA, et al. **Stent-graft placement for wide-neck aneurysm of the vertebrobasilar junction.** *AJNR Am J Neuroradiol* 2004;25:608–10
25. Ionita CN, Suri H, Nataranjian S, et al. **Angiographic imaging evaluation of patient-specific bifurcation-aneurysm phantom treatment with pre-shaped, self-expanding, flow-diverting stents: feasibility study.** *Proc Soc Photo Opt Instrum Eng* 2011;7965:79651H